Available online at www.sciencedirect.com
ScienceDirect
Organic Electronics 8 (2007) 317–324
Organic Electronics
www.elsevier.com/locate/orgel

Control of emission outcoupling in liquid-crystalline fluorescent polymer films

Tae-Woo Lee [a,*], O Ok Park [b], Young Chul Kim [c,*]

[a] Samsung Advanced Institute of Technology, Mt. 14-1 Nongseo-Dong, Giheung-Gu, Yongin-Si, Gyeonggi-Do 449-712, Republic of Korea
[b] Department of Chemical and Biomolecular Engineering, Korea Advanced Institute of Science and Technology, 373-1 Guseong-Dong, Yuseong-Gu, Daejeon 305-701, Republic of Korea
[c] College of Environment and Applied Chemistry, Kyung Hee University, 1 Sochen-ri, Giheung-Gu, Yongin-Si, Gyeonggi-Do 449-701, Republic of Korea

Received 27 February 2006; received in revised form 4 December 2006; accepted 10 December 2006
Available online 29 December 2006

Abstract

We report the improvement of light outcoupling efficiency of thermally annealed thin liquid crystalline light-emitting polymer films. Unlike the generally observed phenomena from thermally annealed fluorescent polymer films, in the liquid-crystalline fluorescent polymer (LCFP) films, the transverse electric waveguide mode was suppressed due to the light scattering by liquid-crystalline domains in the film. In addition, the optical anisotropy of the annealed LCFP was increased. As a result, the light extraction of photoluminescence and electroluminescence emission in the annealed LCFPs was enhanced by ~2 times because the emitted light loss by waveguide was minimized. This approach to improve light extraction by forming scattering domains inside the LCFP film gives an insight to improve the outcoupling efficiency of the EL devices in the viewpoint of the material design and film morphologies without employing external geometric device structures.

PACS: 73.71.Ph; 74.25.Gz

Keywords: Electroluminescence; Emission outcoupling; Liquid crystalline polymer film; Thermal annealing

1. Introduction

Since the first report of polymer light-emitting diode (PLED) based on poly(*p*-phenylenevinylene) in 1990 [1], PLED is rapidly approaching commercialization to full color flat or flexible panel display. However, their poor luminescent efficiency as well as operation instability still remains significant hindrances to their commercialization in full color panel displays. Therefore, improving the external quantum efficiency (η_{ex}) of organic/polymer LEDs is one of the key issues in recent researches of organic LEDs because the internal quantum efficiency (η_{in}) is the intrinsic property of an emitting material and it is now close to the theoretical limit

* Corresponding authors. Tel.: +82 31 280 6765; fax: +82 31 280 6725.
E-mail addresses: taew.lee@samsung.com, taew.lee@yahoo.co.kr (T.-W. Lee), kimyc@khu.ac.kr (Y.C. Kim).

1566-1199/$ - see front matter © 2006 Elsevier B.V. All rights reserved.
doi:10.1016/j.orgel.2006.12.003

[2,3]. η_{ex} can be further improved by increasing the light outcoupling efficiency (ξ) in the devices ($\eta_{ex} = \xi\eta_{in}$) [4,5]. ξ in conventionally constructed organic LEDs is usually as low as ~20% [4,5]. In other words, almost 80% of the light generated in the device is lost due to waveguiding and total internal reflection in the glass substrate generally used in organic LEDs as well as due to re-absorption [4,5]. Therefore, various methods to overcome external efficiency limitations have been proposed to date: for example, introduction of a corrugated surface for Bragg scattering [6], two-dimensional photonic crystals [7], ordered microlens array [8], and self-organized photonic structure of a thin polymer film [9] in the device. The common feature of above methods is to expand the escape cone of the substrate and to suppress the waveguide mode by adding additional photonic structures outside or inside the device. Thus they all need additional patterning processes. In this work, however, we report the enhancement of outcoupling of photoluminescence (PL) and electroluminescence (EL) from liquid-crystalline blue-emitting polymer films by forming liquid crystalline domains inside the film via thermal annealing at nematic–isotropic phase transition temperature (T_{NI}) without employing additional photonic structures. Once liquid crystalline multi-domains by thermal annealing at T_{NI} have been grown inside liquid-crystalline thin films, they can effectively suppress the waveguide mode. As a result, the waveguiding loss of emitted light is reduced due to the light scattering and thus higher external device efficiency is obtained. This approach gives an insight to improve the outcoupling efficiency in the viewpoint of material design and film morphology without using external geometric device structures.

The thermal treatment of EL polymer films at higher temperatures above the glass transition temperature of the material is known to induce interchain emission species and lowering of fluorescence efficiency [10,11]. When the thermal annealing was done before the metal electrode deposition, the device gave a little lower efficiency but demonstrated higher operating stability due to the enhanced packing density of polymer chains [12]. Therefore, if we can obtain a higher external luminous efficiency from the devices comprising thermally annealed polymer emitting films, the device stability at the same luminance can also be further improved since the driving current is lowered for the same device. Nowadays, blue polymer LEDs still have much poorer operational stability compared with the green and red devices. Therefore, it is quite necessary to develop highly stable blue-emitting polymers to expedite the commercialization of full color PLED displays. As a prospective blue-emitting material for PLEDs, polyfluorenes (PFs) have been investigated because they display extremely high luminescence efficiencies with emission wavelengths primarily in the blue spectral region. In addition, polarized electroluminescence from aligned liquid crystalline PFs can be realized [13,14]. However, it has been reported that PFs generate undesired excimer emission [15] or keto emission (a lower energy emission due to keto-defect) [16] due to the strong chain interaction when the PF films were annealed above the glass transition temperature. In contrast, we found that the thermal annealing of LCFP films can improve the outcoupling efficiency of luminescence without generating strong excimer emission or keto emission.

2. Experimental

The PBSDHFS films with varying thickness were spincast from the chlorobenzene solution. The PL spectra of the specimens were measured using an ISS PC1 photon counting spectrofluorometer. The thermal characteristics and the liquid crystallinity of poly(2,7-bis(*p*-stiryl)-9,9′-di-*n*-hexylfluorene sebacate) (PBSDHFS) were examined by employing a Perkin Elmer Pyris 1 differential scanning calorimeter and a Leitz Ortholux II polarized optical microscope equipped with a hot stage, respectively. The films are also spincast on the top of the O_2-plasma-treated indium-tin-oxide (ITO)-coated glass substrates for EL devices. The film thicknesses were averaged after measuring several times by a TENCOR P-10 surface profiler and controlled to be constant. The thickness was calibrated from the UV absorbance for unannealed and annealed films, independently. Aluminum was deposited on the top of the blend film under a high vacuum (10^{-6} torr) and used as the cathode. EL spectra were measured using an ISS PC1 Photon Counting Spectrofluorometer. The spectroscopic refractive index was determined using a dual-beam reflectometer SCI, FilmTek 4000.

The PBSDHFS/poly(9,9-di-*n*-hexyl fluorenediyl-vinylene-*alt*-1,4-phenylenevinylene) (PDHFPPV) blend (98:2 by wt.) films were spincast from the chrolobenzene solution for amplified spontaneous emission study and were photo-pumped with 1 Hz,

800 ps pulses at 337.1 nm generated by a nitrogen laser. The pumping energy was controlled using a set of calibrated neutral density filters. The pumping beam was focused on $1 \times 5\ mm^2$ of the specimen and the emission from the film edge was collected by a Minolta CS1000 spectrofluorometer.

3. Results and discussion

A fluorene-based light-emitting polymer, PBSDHFS was synthesized as reported elsewhere [17] and its chemical structure is shown in Fig. 1a. PBSDHFS showed liquid crystallinity with the glass transition temperature of 48 °C and the T_{NI} of 103 °C as illustrated in Fig. 1b.

We annealed the PBSDHFS films with different thicknesses at 103 °C and then investigated their fluorescence characteristics as a function of the film thickness. The annealing was carried out in a vacuum oven to reduce chemical oxidation where the oven temperature was slowly increased from room temperature to 103 °C for 30 min and kept at 103 °C for 30 min. Before annealing, the film is amorphous and does not have liquid crystalline domains. We did not observe any fluorescence from the unannealed pristine films via a cross polarized fluorescence optical microscope as Fig. 2a shows. But after annealing, the formation of the nematic liquid crystal domain of PBSDHFS was observed by the cross-polarized fluorescence optical microscope as Fig. 2b shows [18]. Actually, although we tried to figure out the liquid crystalline domain size after thermal annealing with the function of the film thickness, we could not observe the domain size clearly due to the resolution limit of the optical microscope. In addition, the cross-polarized fluorescence from the annealed thin films of 50–100 nm thickness was not clearly observed. However, as the film thickness increases above 100 nm, it was getting easier to observe the liquid-crystalline

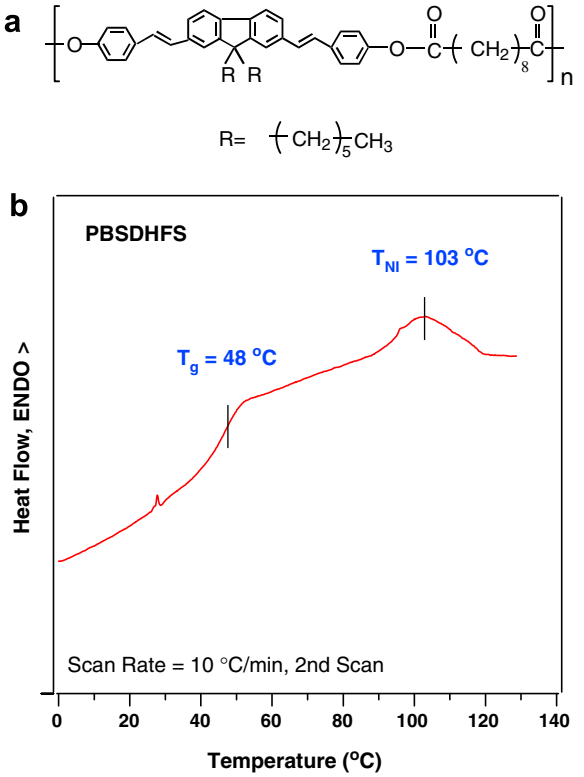

Fig. 1. (a) The chemical structure of poly(2,7-bis(*p*-stiryl)-9,9′-di-*n*-hexylfluorene sebacate) (PBSDHFS). (b) The glass transition temperature (T_g) and the nematic-to-isotropic transition temperature (T_{NI}) determined by differential scanning calorimetry. The PBSDHFS film showed liquid crystallinity with the glass transition temperature of 48 °C and the nematic-to-isotropic transition temperature of 103 °C.

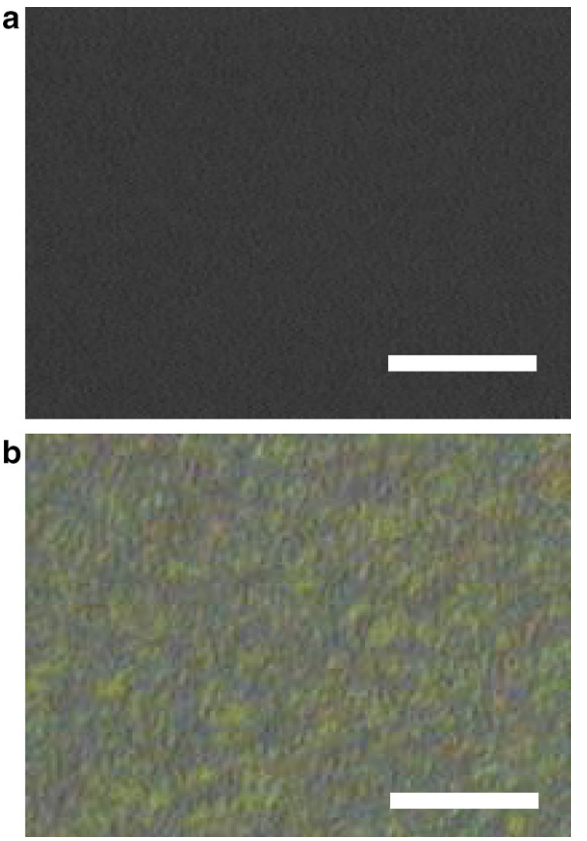

Fig. 2. The cross-polarized fluorescence microscope images for: (a) the unannealed film; (b) the annealed film. The film thickness was ~200 nm. The scale bars are 10 μm.

multi-domains from the cross-polarized fluorescence microscope. Therefore, we speculate that the domain size could increase linearly as the film thickness increase. To find out another evidence of the multi-domain formation, we tried to observe the surface morphology by atomic force microscopy as Fig. 3 shows. Unlike the generally observed surface phenomena for the thermally annealed amorphous films (i.e. smoother surface) [10], the thermally annealed PBSDHFS films have more rough surface than the pristine film, which implies that liquid crystalline multi-domains are formed. The more precise morphological observation of the growth of the nematic liquid crystalline domains in the two-dimensionally confined thin film geometry with varying the film thickness is currently our research topic.

We observed the PL intensities from the films at 90° with respect to the excitation monochromatic light incident on the film at 40° without using an integration sphere in order to compare relatively the outcoupled light intensity of the annealed films

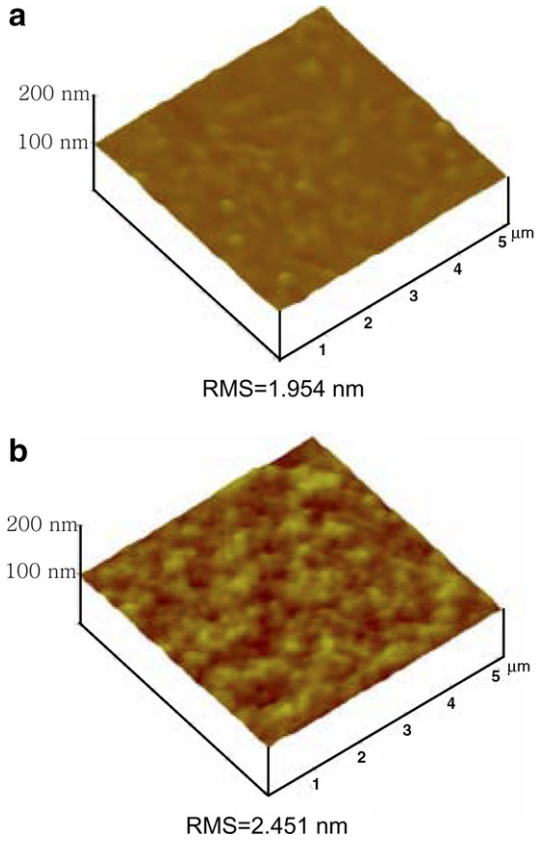

Fig. 3. Atomic force microscope images for: (a) the unannealed film; (b) the annealed film. The film thickness was ~200 nm.

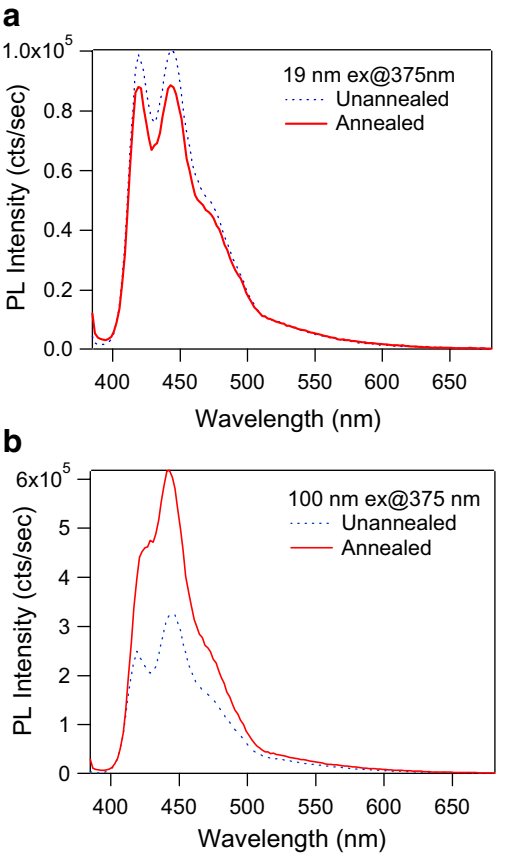

Fig. 4. The PL Spectra of the PBSDHFS films before and after the annealing at 103 °C, measured while being excited at 375 nm: (a) the 19 nm-thick film and (b) the 100 nm-thick film.

with that of the unannealed film. By the thermal annealing, the PL intensity of the 19 nm-thick PBSDHFS film was decreased by ~10% (Fig. 4a), which was generally observed in annealed fluorescent polymer films [10]. The PL intensity reduction comes from the interchain interactions in the annealed films [10]. For the 100 nm-thick film, however, the PL intensity was almost doubled after the thermal annealing (Fig. 4b). In addition, we did not observe any undesired spectral broadening over lower energy emission band that had been observed for polyfluorenes due to the excimers or keto defects formation [15,16]. It is worth noting that the full-width at half maximum (FWHM) of the PL spectrum was reduced from 58 to 46 nm by the annealing.

We plotted the PL intensity of the PBSDHFS films as a function of the film thickness before and after the annealing as Fig. 5a shows. The ratio of the PL intensities measured before and after the

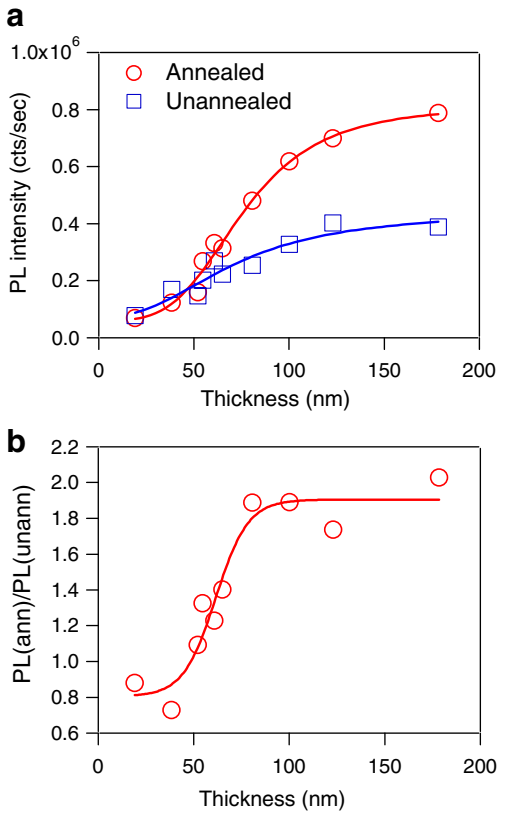

Fig. 5. (a) The PL intensities of the PBSDHFS films before and after the annealing as a function of the film thickness. (b) The ratio of the PL intensities measured before and after the annealing as a function of the film thickness.

annealing was also shown as a function of the film thickness in Fig. 5b. The PL intensity ratio tends to increase as the film thickness exceeds ~50 nm and then saturates after the thickness reaches ~80 nm where the PL intensity is almost doubled. We consider this PL intensity increase by the annealing originates from the liquid-crystalline nature of the film material because the liquid-crystalline domains in the PBSDHFS films will grow up by annealing. The PL intensity increase for the films thicker than 50 nm indicates that the light scattering by the domains starts to be effective when the film thickness exceeds ~50 nm to suppress the waveguide mode. The light scattering inside the film waveguide changes the direction of the propagating light to escape the waveguide. We found that the cut-off thickness of the zero-order transverse electric (TE) mode waveguiding ($d_{c,TE}$) is close to 50 nm. $d_{c,TE}$ is expressed by the following equation that represents the zero-order TE-mode of waveguiding [19].

$$d_{c,TE} = \frac{\lambda}{2\pi\sqrt{n_p^2 - n_s^2}} \tan^{-1}\left(\sqrt{\frac{n_s^2 - n_c^2}{n_p^2 - n_s^2}}\right) \quad (1)$$

where n_p, n_s, and n_c are the refractive indices of the polymer (PBSDHFS), substrate (glass), and cladding layer (air), respectively, and λ is the wavelength. $d_{c,TE}$ was obtained to be 54 nm from the Eq. (1) with the known parameters ($n_s = 1.5$, $n_c = 1.0$, $n_p = 1.83$ at 430 nm). Therefore, the light scattering within the waveguide becomes effective when the film is thicker than the $d_{c,TE}$ of 54 nm. This implies that although the film is much thinner than the wavelength of visible light, the lateral dimension of the nematic liquid crystal domains may grow to be large enough to scatter visible light in the TE-mode waveguiding along the substrate. The detailed growth mechanism of the lateral liquid crystalline domain size inside the confined geometry and the estimation of the lateral liquid crystalline domain size with the function of film thickness are beyond the scope of this paper and currently another research subject. Our approach is unique in that the fluorescent film itself acts as a light scattering medium as a single polymer film without adding an optical structure or a layer on the surface. Other approaches using Bragg scattering in a laterally corrugated microstructures [6] or phase separated microstructures by self-organization using a polymer blend [9] cause a rough device surface which can be a potential source to deteriorate a device long-term stability due to uneven electric field.

In order to confirm the suppression of the waveguide mode in the EL device, we fabricated the devices of the structure of indium-tin-oxide (ITO)/PBSDHFS/Al with the annealed and unannealed PBSDHFS films. As Fig. 6a shows, the EL intensity of the device based on the annealed film was also doubled at the same bias voltage (11 V) and the FWHM of the EL spectrum was also narrowed. To date, we have generally observed that the EL devices based on thermally annealed EL film above the glass transition temperature have shown lower device quantum efficiency [10], However, as the inset of Fig. 6b shows, the maximum EL quantum efficiency of the device with the annealed film is ~2.8 times higher than that of the one with the unannealed film although the current versus voltage characteristics are similar as shown in Fig. 6b. Without any geometrical modification of the device, the outcoupling of the light intensity could be enhanced by the formation of the lateral liquid crystalline

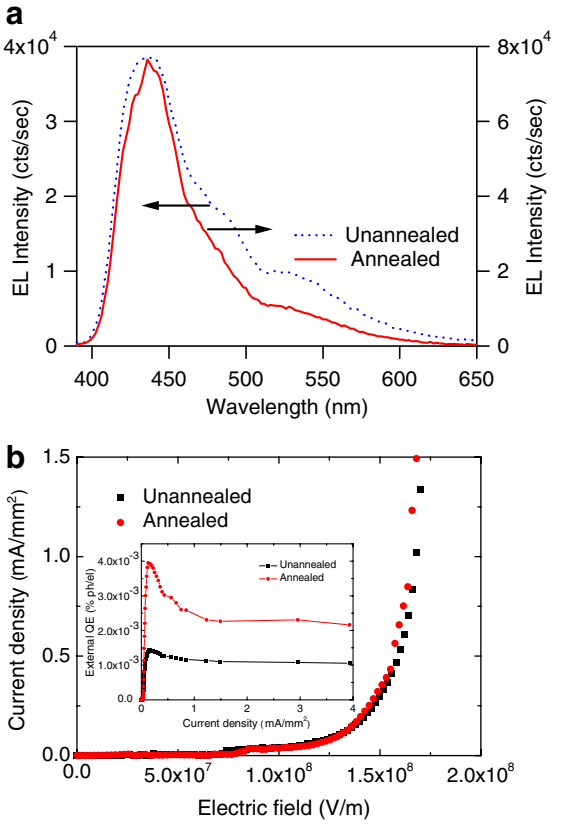

Fig. 6. (a) The EL spectra of the ITO/PBSDHFS/Al devices based on the annealed and unannealed PBSDHFS films, measured at the operating voltage of 11 V. (b) The current density versus electric field characteristics of the ITO/PBSDHFS/Al devices. The inset shows the external EL quantum efficiency (Q.E.) as a function of the current density. The 100 nm PBSDHFS film became thinner (95 nm) after thermal annealing. Thus we showed electric field (V/m) on the x axis.

domains via the thermal annealing only. Beside the fact that we doubled the extracted light intensity, the device operation lifetime also can be much more improved if we drive the device at the lowered current density for the same luminance level. For example, when we apply 2.0 as the conversion acceleration factor of the lifetime for the half reduction of the luminance level, the device lifetime can be 4 times improved [20,21]. Therefore, this simple light extraction method can be useful to improve the efficiency and the lifetime of the polymer LEDs based on LCFPs.

In order to reconfirm that the waveguide mode was suppressed by the formation of the liquid crystalline domain via the annealing, we examined the edge emission from the annealed and unannealed films. The excitation geometry is shown in Fig. 7a. When we photo-excited the 15 nm-thick film before and after the annealing, the PL intensity was a little lowered after the annealing but the PL spectrum remained almost unchanged, which are very similar to the results shown in Fig. 4a. This indicates that the PL characteristics of the edge emission from the films thinner than $d_{c,TE}$ are not different from those of the normal emission. In contrast, the PL intensity of the edge emission from the 100 nm-thick annealed film was much lower than that from the unannealed film of the same thickness as Fig. 7c shows, which suggests that the waveguide mode was largely suppressed due to the light scattering inside the annealed film. The amplified spontaneous emission from the edge of the thin fluorescent films on the substrates with low refractive index such as glass or quartz has been reported to date [18,22,23]. We observed a low-threshold amplified spontaneous emission (~20 nJ/cm^2/pulse) in the blend film of PBSDHFS with 2 wt% PDHFPPV as Fig. 7d shows [17]. However, with the annealed LCFP film, we did not observe the amplified spontaneous emission at a very high excitation energy (600 μJ) due to the waveguide mode suppression while the unannealed film showed a gain narrowing even at much lower excitation energy (~24 nJ). This also supports that the waveguide mode is largely suppressed in the annealed LCFP films due to light scattering by the liquid crystalline domains. Thus the amplified spontaneous emission of the annealed fluorescent film on glass can not occur since emitting light can not effectively travel the film slab waveguide.

We also tried to observe optical anisotropy of the LCFP film before and after the thermal annealing. As Fig. 8 shows, it is interesting to observe that the film anisotropy (Δn) was increased after thermal annealing although the overall refractive index values were reduced. Hence, the total intensity coupled out of the device increases when the emitters are aligned in the plane compared with an isotropic orientation [5]. This is possibly because that annealing changes the director orientation of the annealed liquid crystalline films. We optically simulated the outcoupled luminescence yield from the device when we assume that the emitting dipoles aligned only in the plane (i.e. no out-of-plane emitting dipoles). In this case, the luminescence yield was improved by ~49% compared with the perfect isotropic orientation [24]. Other literature also reported that the ~58% improvement of outcoupling efficiency for Al

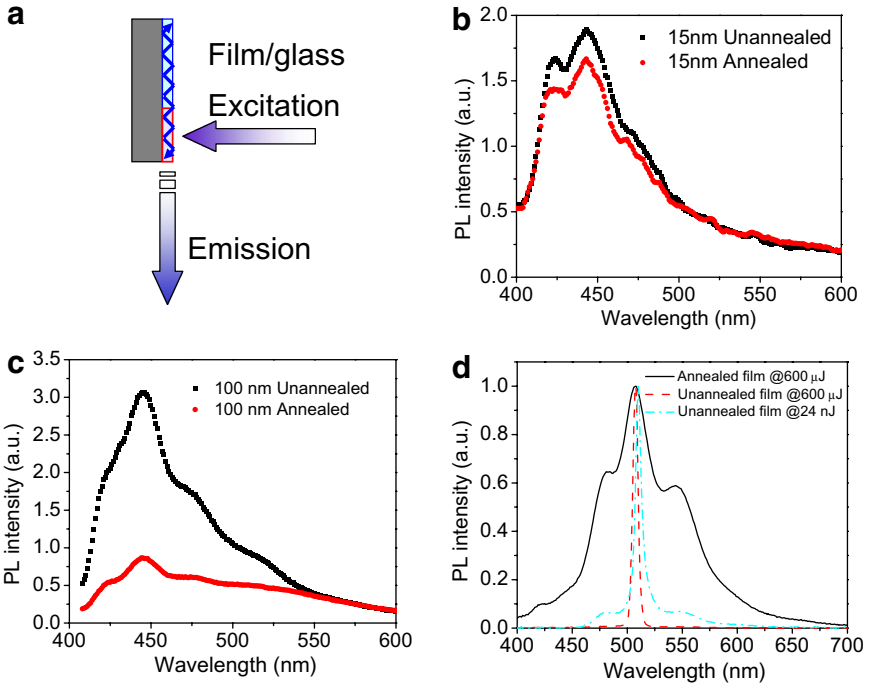

Fig. 7. The PL characteristics of the edge emissions from the PBSDHFS films before and after the annealing measured while exciting the films at the normal incident angle: (a) the 15 nm-thick film excited by the 370 nm monochromatic beam; (b) the 100 nm-thick film excited by the 370 nm monochromatic beam; (c) the 100 nm-thick film excited by the 337.1 nm pulsed N_2 laser. The film contains 2 wt% of PDHFPPV.

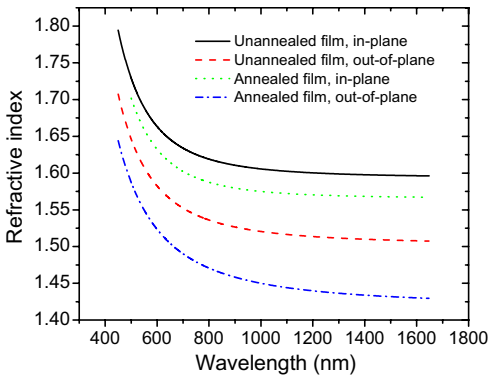

Fig. 8. The in-plane and out-of-plane refractive index with the function of the wavelengths for the unannealed and annealed films.

devices based on the emitting film with only in-plane dipoles compared with that with the isotropic dipoles [5]. Although, in the annealed film (with liquid crystalline domain), the emitting dipoles was more aligned in the plane compared with those in the unannealed film (without liquid crystalline domain), the outcoupled light improvement by the difference in optical anisotropy between the unannealed and the annealed film should be much less than ~49%. Therefore, the ~2 time improvement in light extraction mainly originated from the light scattering inside the films due to the multi-domains.

4. Conclusion

Thermal annealing for fluorescent polymers, especially polyfluorene derivatives, generally give rise to the generation of a lower energy emission (excimer or keto emission) and the lower fluorescence yield. However, we found that the improvement of light outcoupling efficiency above the cut-off thickness of TE waveguide can be realized in thin LCFP films by the formation of the liquid crystalline domains via thermal annealing. The TE waveguide mode was suppressed due to the light scattering by liquid-crystalline multi-domains in the film. As a result, the external PL and EL efficiency was enhanced by ~2 times above the cut-off thickness of TE waveguide mode. This approach to form liquid crystalline multi-domains in LCFP film by thermal annealing gives an insight to

improve the light extraction yield in the EL devices in the viewpoint of material design and film morphology without employing external geometric device structures.

Acknowledgements

We acknowledge Prof. B.J. Schwartz for helpful discussion and Dr. H. Jeong for optical calculation. This work was supported by Grant No. R01-2005-000-10852-0 from the Basic Research Program of the Korea Science & Engineering Foundation.

References

[1] J.H. Burroughes, D.D.C. Bradley, A.R. Brown, R.N. Marks, K. Mackay, R.H. Friend, P.L. Burns, A.B. Holmes, Nature 347 (1990) 539.
[2] C. Adachi, M. Baldo, S.R. Forrest, M.E. Thompson, J. Appl. Phys. 90 (2001) 5048.
[3] Y. Cao, I.D. Parker, G. Yu, C. Zhang, A.J. Heeger, Nature 397 (1999) 414.
[4] S.R. Forrest, D.D.C. Bradley, M.E. Thompson, Adv. Mater. 13 (2003) 1043.
[5] J.-S. Kim, P.K.H. Ho, N.C. Greenham, R.H. Friend, J. Appl. Phys. 88 (2000) 1073.
[6] (a) B.J. Matterson, J.M. Lupton, A.F. Safonov, M.G. Salt, W.L. Barnes, I.D.W. Samuel, Adv. Mater. 13 (2001) 123; (b) J.M. Ziebarth, A.K. Saafir, S. Fan, M.D. McGehee, Adv. Funct. Mater. 14 (2004) 451.
[7] Y.R. Do, Y.C. Kim, Y.-W. Song, C.-O. Cho, H. Jeon, Y.-J. Lee, S.-H. Kim, Y.-H. Lee, Adv. Mater. 15 (2003) 1214.
[8] S. Möller, S.R. Forrest, J. Appl. Phys. 91 (2002) 3324.
[9] (a) G. Fichet, N. Corcoran, P.K.H. Ho, A.C. Arias, J.D. MacKenzie, W.T.S. Huck, R.H. Friend, Adv. Mater. 16 (2004) 1908; (b) N. Corcoran, P.K.H. Ho, A.C. Arias, J.D. Mackenzie, R.H. Friend, G. Fichet, W.T.S. Huck, Appl. Phys. Lett. 85 (2004) 2965.
[10] T.-W. Lee, O.O. Park, Adv. Mater. 12 (2000) 801.
[11] (a) S.A. Jenekhe, J.A. Osaheni, Science 265 (1994) 765; (b) S.A. Jenekhe, Adv. Mater. 7 (1995) 309.
[12] (a) J. Kim, J. Lee, C.W. Han, N.Y. Lee, I.-J. Chung, Appl. Phys. Lett. 82 (2003) 4238; (b) T.-W. Lee, M.-G. Kim, S.Y. Kim, S.H. Park, O. Kwon, T. Noh, T.-S. Oh, Appl. Phys. Lett. 89 (2006) 123505.
[13] M. Grell, W. Knoll, D. Lupo, A. Meisel, T. Miteva, D. Neher, H.-G. Nothofer, U. Scherf, A. Yasuda, Adv. Mater. 11 (1999) 671.
[14] M. Grell, D.D.C. Bradley, Adv. Mater. 11 (1999) 895.
[15] J.-I. Lee, G. Klaerner, R.D. Miller, Chem. Mater. 11 (1999) 1093.
[16] E.J.W. List, R. Guentner, P.S. de Freitas, U. Scherf, Adv. Mater. 14 (2002) 374.
[17] Y.C. Kim, H.N. Cho, D.Y. Kim, J.M. Hong, N.W. Song, D. Kim, C.Y. Kim, Polymer (Korea) 24 (2000) 211.
[18] Y.C. Kim, T.-W. Lee, O.O. Park, C.Y. Kim, H.N. Cho, Adv. Mater. 13 (2001) 646.
[19] M. Marcuse, Theory of Dielectric Waveguides, Academic, New York, 1974 (Chapter 1).
[20] J. Burroughes, PLED: A Display Technology, ASIA DISPLAY/IMID'04, 23–27 August 2004, Daegu, Korea, Session 11.3.
[21] Although we did not test the operational stability with a function of time, we found that the annealed devices are more stable against the electrical current. The unannealed devices failed at the current density of 1.34 mA/mm^2. However, the annealed devices endured even higher current density (7.62 mA/mm^2).
[22] R. Gupta, M. Stevenson, A. Dogariu, M.D. McGehee, J.Y. Park, V. Srdanov, A.J. Heeger, Appl. Phys. Lett. 73 (1998) 3492.
[23] T.-W. Lee, O.O. Park, D.H. Choi, H.N. Cho, Y.C. Kim, Appl. Phys. Lett. 81 (2002) 424.
[24] The calculation was done by the optical simulator, Haemosu which was developed in Samsung SDI.